

Recommended Practices for Calibrated Millimeter-Wave Modulated-Signal Measurements

Paritosh Manurkar^{1,2}, Joshua M. Kast^{2,3}, Dylan F. Williams², Robert D. Horansky², Daniel G. Kuester²,
Kate A. Remley²

¹University of Colorado, Boulder, USA, ²National Institute of Standards and Technology, Boulder, USA,
³Colorado School of Mines, Golden, USA

Abstract — In a millimeter-wave modulated-signal measurement system with several calibration reference planes, we want the measured signal to be a close replica of the ideal signal at the reference plane which connects the near-ideal measured signal to subsequent applications, such as, over-the-air measurements. Recommended practices to transfer reference planes in such a situation are described here to ensure availability of a calibrated signal at the correct reference plane. Our work also highlights and demonstrates design choices to minimize the impact of receiver mismatch when using the calibrated modulated signal for subsequent applications.

Index Terms — Digitally modulated signals, error vector magnitude, predistortion, reference planes, uncertainty analysis, wireless systems.

I. INTRODUCTION

Modulated-signal sources at millimeter-wave frequencies may be calibrated and then used in a laboratory setting to calibrate receivers. We have previously demonstrated traceable measurements of error vector magnitude (EVM) using calibrated modulated-signal sources [1], [2] along with complete uncertainty analyses using the NIST Microwave Uncertainty Framework [3]. To produce a faithful replica of the designed signal, the nonidealities in the source hardware are taken into account during the signal-generation process. This task is accomplished by predistorting the signal [4] measured by a calibrated receiver until a low nominal EVM (e.g., less than 1.5%) is reached. The errors introduced by the receiver are first corrected for while predistorting the signal and residual errors are accounted for in the uncertainty analysis. This low-EVM signal can be used for subsequent applications, such as performing over-the-air (OTA) measurements.

The reference plane where the signal is predistorted can be different from the reference plane where the measurements are performed making such measurements and the associated uncertainty analyses quite complicated. Therefore, transferring the reference plane correctly impacts the accuracy of signal produced for further applications. This paper proposes recommended practices for performing calibrated millimeter-wave modulated-signal measurements with a focus on the reliable transfer of reference planes. We also make an important recommendation for minimizing impedance mismatch in the modulated-signal source setup. These practices are recommended when performing calibrated

millimeter-wave modulated-signal measurements in a laboratory setting.

II. MILLIMETER-WAVE MODULATED-SIGNAL SOURCE: MEASUREMENT AND UNCERTAINTY ANALYSIS

The main principles for calibrating wideband, millimeter-wave modulated-signal sources along with the measurement procedure, postprocessing, and uncertainty analysis have already been published in detail [1], [2]. To summarize briefly, we provide an example of a 44-GHz source here for completeness. A signal generator produces a 10-GHz tone which serves as the reference clock for an arbitrary waveform generator (AWG). The AWG then triggers an amplitude- and phase-calibrated equivalent-time sampling oscilloscope. The timebase distortion correction waveforms are also generated by the signal generator. Finally, the 10-GHz tone serves as the local oscillator (LO) for the upconverter which is multiplied by four, amplified, filtered, then mixed with the modulated signal generated by the AWG at an IF of 4 GHz to produce the RF modulated signal at 44 GHz. In this way, the entire measurement setup is referenced to the 10-GHz tone as opposed to the more commonly used 10-MHz reference. The modulated millimeter-wave signal is attenuated (to improve impedance mismatch) and fed through an isolator before passing through an output cable for measurement on the calibrated equivalent-time sampling oscilloscope or for use in other applications such as OTA measurements. The equivalent-time sampling oscilloscope is calibrated in phase using a photodiode standard, which in turn is calibrated by the NIST electro-optic sampling (EOS) system [5]–[7], and can be calibrated in amplitude through a traceable power sensor. The entire setup is mismatch corrected.

To obtain a low EVM signal, we must predistort the signal uploaded to the AWG to account for the various nonidealities in the system. Predistorting the ideal signal is accomplished by iteratively estimating the transfer function of the system and compensating for it in the signal to be uploaded on the AWG. The iterative process accounts for both linear and nonlinear distortion in the modulated-signal source [4]. We choose four iterations of the predistortion since the difference between computed EVM values after four iterations is typically quite low (~0.1%) and it has minimal impact on the final uncertainty analysis. The final predistorted signal minimizes

EVM measured directly from the source, that is, the measured signal is a close replica of the ideal signal at the chosen predistortion reference plane. For predistortion, each oscilloscope measurement is corrected for distortion in oscilloscope’s timebase and for drift followed by source mismatch, oscilloscope mismatch and response corrections. Additionally, to obtain the EVM distribution, the uncertainties related to mismatch and oscilloscope response are also accounted for in the uncertainty analysis performed in the NIST Microwave Uncertainty Framework. The framework performs both Monte Carlo and sensitivity analyses. The Monte Carlo analysis is used to propagate errors through nonlinear process, such as EVM. The final output of the analysis is an EVM distribution which shows the nominal EVM (in which the receiver nonidealities have been minimized through predistortion), the Monte Carlo mean EVM (which accounts for the receiver uncertainty), and upper and lower 95% confidence limits for the Monte Carlo analysis.

III. PREDISTORTION AND CHOICE OF REFERENCE PLANE

Before we predistort the signal, we need to decide upon the correct reference plane for the subsequent application. Fig. 1(a) shows a typical millimeter-wave measurement setup.

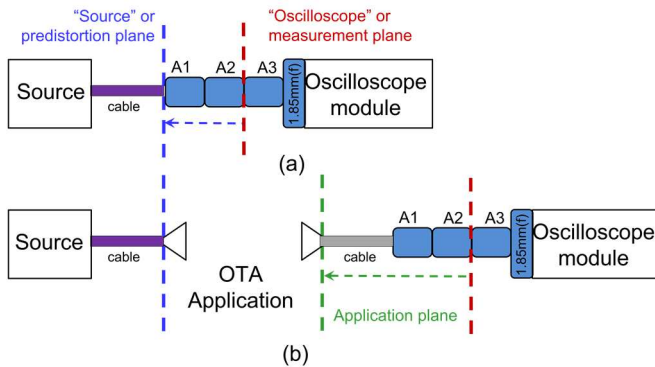


Fig. 1. Typical millimeter-wave measurement on a calibrated equivalent-time sampling oscilloscope. (a) The measurement is performed at the “oscilloscope” plane which may need to be transferred to the “source” plane. (b) The calibrated signal at the end of the cable is connected to an OTA application. The measurement is again performed at the “oscilloscope” plane, and then transferred to the “application” plane.

Typically, the source plane corresponds to the predistortion plane (blue), and the oscilloscope plane corresponds to the measurement plane (red). Not keeping track of these reference planes will produce two quite different signals as will be shown in Fig. 2(b). We want our near-replica of the ideal signal at the predistortion or source plane such that the low-EVM signal obtained here can be directly connected to, for example, the transmit antenna in an OTA experiment.

However, the signal is measured at the oscilloscope reference plane which necessitates de-embedding of the two adapters (A1 and A2 in this case) to transfer the reference

plane to the source plane. As will be shown, de-embedding is crucial at millimeter-wave frequencies. At lower frequencies, such adapter de-embedding may not have a significant impact on the EVM of the generated signal.

To de-embed the adapters, we used the Cascade tool employed in the NIST Microwave Uncertainty Framework. During the predistortion process, the de-embedding of adapters occurs in postprocessing without applying the uncertainty analysis. If S^{A1} and S^{A2} are the scattering parameter matrices of the adapters A1 and A2, respectively, then the scattering parameter matrix S of the cascaded adapter can be calculated as follows:

$$S_{11} = S_{11}^{A1} + \frac{S_{12}^{A1} S_{21}^{A2} S_{11}^{A1}}{D} \quad (1)$$

$$S_{22} = S_{22}^{A2} + \frac{S_{21}^{A2} S_{12}^{A1} S_{22}^{A2}}{D} \quad (2)$$

$$S_{12} = \frac{S_{12}^{A1} S_{12}^{A2}}{D} \quad (3)$$

$$S_{21} = \frac{S_{21}^{A2} S_{21}^{A1}}{D} \quad (4)$$

where

$$D = 1 - S_{11}^{A2} S_{22}^{A1} \quad (5)$$

When D is zero, the Microwave Uncertainty Framework makes D a small number, say, 10^{-12} , to ensure that (1)–(4) are non-singular. Eqs. (1)–(5) are subsequently used to obtain the calibrated signal at the source plane by cascading the source mismatch, the cascaded adapters, the oscilloscope mismatch, and response with the uncalibrated signal.

Fig. 2(a) shows the source mismatch at the source reference plane (blue) and the oscilloscope reference plane (red). The lines are the Monte Carlo estimates whereas the shaded regions are the 95% confidence intervals. It can be seen clearly that both the source mismatch and the associated uncertainties change by several decibels with the adapters, thereby, highlighting the importance of de-embedding the adapters during the predistortion process. The change in the Monte Carlo mean EVM and the 95% confidence limits is also evident when the adapters are de-embedded to transfer the reference plane from the oscilloscope to the source plane.

For this work, we used the IEEE 1765 Reference Waveform 1 which does not include any distortion characteristics [8], [9] and predistorted it to the source reference plane in four iterations followed by several repeat measurements of the final predistorted signal [10]. The nominal EVM for each measurement was calculated using the IEEE 1765 Baseline EVM Algorithm [8], [9].

We input into the NIST Microwave Uncertainty Framework the uncertainties associated with the source mismatch, the oscilloscope mismatch and response, the cascaded adapters calculated above, cable bending, and the repeat measurements of the final predistorted signal. We then calibrated the measured signal at the oscilloscope reference plane and transferred it to the source reference plane. We computed the uncertainty in EVM using 1000 Monte Carlo samples, with

results shown in Fig. 3, for the calibrated signal at the source reference plane.

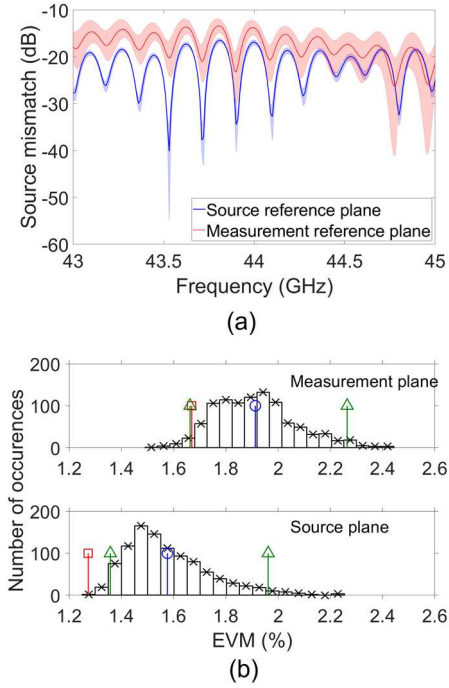


Fig. 2: Choosing the appropriate reference plane is important for both (a) the source mismatch and the associated uncertainties (shaded areas are 95% confidence intervals) and (b) the computed EVM distribution upon uncertainty analysis (red square: nominal EVM, blue circle: Monte Carlo mean, green triangles: 95% confidence limits).

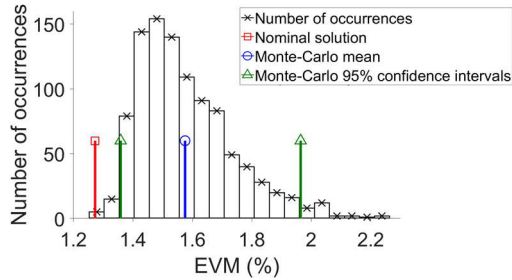


Fig. 3: Uncertainty in measured EVM of IEEE 1765 Reference Waveform 1 (expected EVM of $\approx 0\%$). The nominal EVM (red square) is the EVM value that was obtained by predistorting out both the residual source and receiver hardware errors. When the receiver hardware errors are accounted for in the uncertainty analysis, the EVM obtained in the measurement is denoted by the Monte Carlo mean (blue circle) along with the 95% confidence limits (green triangles)

IV. OSCILLOSCOPE MISMATCH

The oscilloscope modules used for millimeter-wave measurements can create reflections back to the source reference plane due to relatively high mismatch at millimeter-wave frequencies. We show in Fig. 4(a) the measured

mismatch for our 50-GHz and 67-GHz oscilloscope modules used for millimeter-wave measurements. The figure shows a bandwidth of 50 GHz for comparison. The 67-GHz oscilloscope, used here, exhibits mismatch at 44 GHz that is higher than that at lower frequencies. The effect of reflections caused by such high mismatch can be prominently seen when a device is connected to the source’s output. Therefore, we designed a setup similar to Fig. 1(b) to simulate an OTA path which enabled us to study the effects of receiver mismatch on EVM measurements.

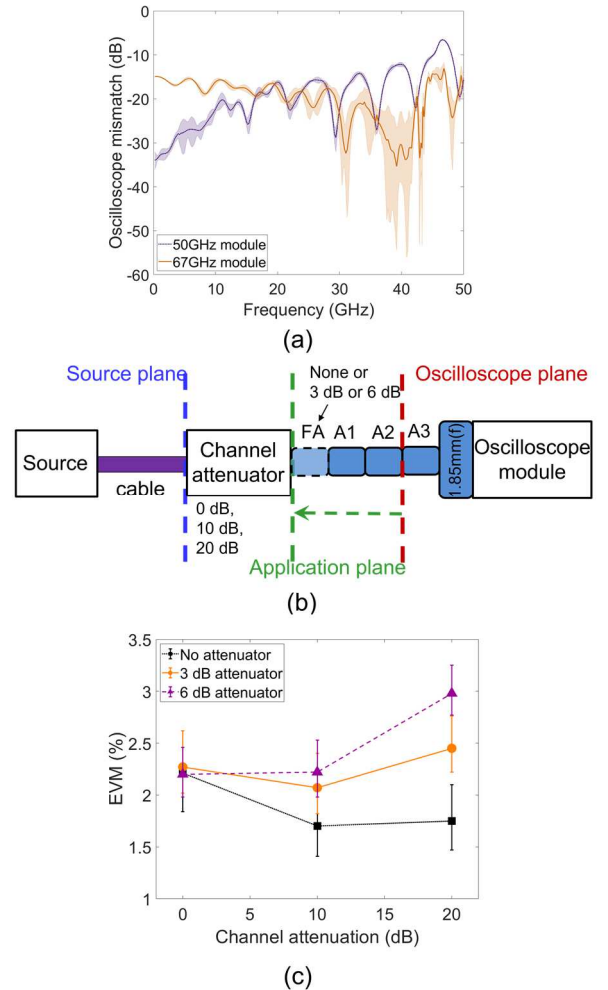


Fig. 4: (a) Measured mismatch for two oscilloscope modules. The lines are the Monte Carlo mean; the 95% confidence intervals depicted by the shaded area. (b) Simulating an OTA setup with a waveguide attenuator. A fixed attenuator (FA) is inserted to account for high oscilloscope mismatch. (c) The effect of high oscilloscope mismatch on EVM measurements with no fixed attenuator (black squares), and with added fixed attenuators of 3 dB and 6 dB (orange circles and purple triangles, respectively).

We connected the source’s output cable to a variable waveguide “channel attenuator” simulating an OTA channel as shown in Fig. 4(b) and measured a signal that was predistorted to the source reference plane. The measured

The authors would like to thank the Working Group members of the IEEE 1765-2022 standard, Recommended Practice for EVM Measurement and Uncertainty Evaluation.

REFERENCES

signal was transferred from the oscilloscope (red dashed line) to the application reference plane (green dashed line) followed by a complete uncertainty analysis at each channel attenuation value. We performed these measurements without any fixed attenuator (FA in Fig. 4b) at three channel attenuations of 0 dB, 10 dB, and 20 dB. These data points are shown in Fig. 4(c) with black squares.

Because the source's output was being attenuated by the channel attenuator, we would have expected the EVM at 10 dB and 20 dB of channel attenuation to be *higher* than the EVM at 0 dB since EVM is (ideally) inversely proportional to the square root of the signal-to-noise ratio [11], [12]. Instead, we observed that the EVM at 10 dB and 20 dB channel attenuation was lower than that at 0 dB channel attenuations. We attribute this effect to the reflections between the channel attenuator and the oscilloscope module.

To reduce these reflections, we inserted a fixed attenuator between the channel attenuator and the adapter A1 and remeasured the same predistorted signal. With the 3-dB fixed attenuator inserted, we set the channel attenuator to 0 dB, 10 dB, and 20 dB and performed measurements at each value. These data points are shown with orange circles. Then, we removed the 3-dB and inserted the 6-dB fixed attenuator, set the channel attenuator to 0 dB, 10 dB, and 20 dB, and performed measurements at each value. These data points are shown with purple triangles. Ideally, the measured oscilloscope mismatch should be reduced by an amount equal to twice the fixed attenuation. Inserting such attenuation would also lead to an increase in EVM due to the reduction in SNR (approximately $1/\sqrt{\text{SNR}}$) when we increase the channel attenuation. However, Fig. 4(a) shows a high mismatch, and we did not observe the expected increase in EVM for either 0-dB and 3-dB fixed attenuators. Only the 6-dB fixed attenuator resulted in the expected trend of increased EVM (due to reduction in SNR by increasing the channel attenuation).

V. CONCLUSION

In this paper, we have discussed the process for calibrating a modulated-signal measurement and the transfer of the reference planes. We have illustrated this process by transferring a wideband 44-GHz modulated-signal measurement from the oscilloscope plane (red dashed line in Fig.1) to the source plane (blue dashed line in Fig.1), the latter being connected to subsequent applications such as OTA measurements. We have demonstrated through a test application setup where a waveguide attenuator simulated an OTA path that it may be necessary to add an appropriate fixed attenuator before the oscilloscope module and its adapters to minimize the impact of high oscilloscope mismatch at millimeter-wave frequencies. These recommended practices allow increased confidence in calibrated modulated-signal measurements at millimeter-wave frequencies.

- [1] K. A. Remley, D. F. Williams, P. D. Hale, C. Wang, J. Jargon, and Y. Park, "Millimeter-Wave Modulated-Signal and Error-Vector-Magnitude Measurement with Uncertainty," *IEEE Trans. Microw. Theory Tech.*, vol. 63, no. 5, pp. 1710–1720, May 2015, doi: 10.1109/TMTT.2015.2416180.
- [2] P. Manurkar, R. D. Horansky, B. F. Jamroz, J. A. Jargon, D. F. Williams, and K. A. Remley, "Precision Millimeter-Wave-Modulated Wideband Source at 92.4 GHz as a Step Toward an Over-the-Air Reference," *IEEE Trans. Microw. Theory Tech.*, vol. 68, no. 7, pp. 2644–2654, Jul. 2020, doi: 10.1109/TMTT.2020.2983144.
- [3] D. Williams, "On-Wafer Calibration Software," *NIST*, Aug. 05, 2009. <https://www.nist.gov/services-resources/software/wafer-calibration-software> (accessed Apr. 05, 2021).
- [4] K. A. Remley, D. F. Williams, P. D. Hale, and J. A. Jargon, and Y. Park, "Calibrated oscilloscope measurements for system-level characterization of weakly nonlinear sources," in *2014 International Workshop on Integrated Nonlinear Microwave and Millimetre-wave Circuits (INMMiC)*, Apr. 2014, pp. 1–4. doi: 10.1109/INMMiC.2014.6815075.
- [5] T. S. Clement, P. D. Hale, D. F. Williams, C. M. Wang, A. Dienstfrey, and D. A. Keenan, "Calibration of sampling oscilloscopes with high-speed photodiodes," *IEEE Trans. Microw. Theory Tech.*, vol. 54, no. 8, pp. 3173–3181, Aug. 2006, doi: 10.1109/TMTT.2006.879135.
- [6] M. R. Harper, A. J. A. Smith, A. Basu, and D. A. Humphreys, "Calibration of a 70 GHz Oscilloscope," in *2004 Conference on Precision Electromagnetic Measurements*, Jun. 2004, pp. 530–531. doi: 10.1109/CPem.2004.305346.
- [7] H. Füser *et al.*, "Optoelectronic time-domain characterization of a 100 GHz sampling oscilloscope," *Meas. Sci. Technol.*, vol. 23, no. 2, p. 025201, Dec. 2011, doi: 10.1088/0957-0233/23/2/025201.
- [8] "IEEE SA - IEEE 1765-2022," *IEEE Standards Association*. <https://standards.ieee.org/ieee/1765/10560/> (accessed Sep. 06, 2022).
- [9] "Open-Source Repository: IEEE P1765 Recommended Practice for EVM Measurement and Uncertainty Evaluation," *GitLab*. <https://opensource.ieee.org/1765/1765> (accessed Dec. 03, 2021).
- [10] P. Manurkar, C. P. Silva, J. Kast, R. D. Horansky, D. F. Williams, and K. A. Remley, "Reference Measurements of Error Vector Magnitude," in *2022 IEEE/MTT-S International Microwave Symposium - IMS 2022*, Jun. 2022, pp. 1026–1029. doi: 10.1109/IMS37962.2022.9865278.
- [11] H. A. Mahmoud and H. Arslan, "Error vector magnitude to SNR conversion for nondata-aided receivers," *IEEE Trans. Wirel. Commun.*, vol. 8, no. 5, pp. 2694–2704, May 2009, doi: 10.1109/TWC.2009.080862.
- [12] R. A. Shafik, Md. S. Rahman, and A. R. Islam, "On the Extended Relationships Among EVM, BER and SNR as Performance Metrics," in *2006 International Conference on Electrical and Computer Engineering*, Dec. 2006, pp. 408–411. doi: 10.1109/ICECE.2006.355657.